Pedobiological properties of a lignite spoil heap in the Provence coal mine basin (south-east of France)

Stéven Criquet, Mélanie Clouard, Fabio Ziarelli, D Borschneck, Catherine Keller

Pedobiological properties of a lignite spoil heap in the Provence coal mine basin (south-east of France)

Stéven Criquet[a*], Mélanie Clouard[a,b], Daniel Borschneck[b], Fabio Ziarelli[c], Catherine Keller[b]

[(a)] *Aix-Marseille Univ., Faculté des Sciences de Saint-Jérôme, IMBE – Institut Méditerranéen de Biodiversité et d'Ecologie marine et continentale UMR CNRS 7263 - IRD 237 – Systèmes microbiens, Service 452, Avenue Escadrille Normandie-Niemen 13397 Marseille cedex 20, France*

[(b)]*Aix-Marseille Univ., CNRS, IRD, INRAE, CEREGE – Technopole de l'Environnement Arbois-Méditerranée, BP 80, 13545 Aix-en-Provence, Cedex 4, France*

[(c)]*Aix-Marseille Univ., Faculté des Sciences et Techniques de Saint-Jérôme, Spectropole, P.O. Box 512, Avenue Escadrille Normandie Niémen, 13397 Marseille cedex 20, France*

**Corresponding author ; E-mail address:* steven.criquet@imbe.fr*; Postal address:* Site de l'Etoile, FST de St-Jérôme, IMBE, Case 441, Avenue Escadrille Normandie-Niémen, F-13397, Marseille Cedex 20, France

E-mail addresses of co-authors: steven.criquet@imbe.fr (Stéven Criquet), melanie.clouard@dreets.gouv.fr (Mélanie Clouard), borschneck@cerege.fr (Daniel Borschneck), fabio.ziarelli@univ-amu.fr (Fabio Ziarelli), keller@cerege.fr (Catherine Keller)

Declaration of interest: none

Abstract

The aim of this study was to investigate the bio-physico-chemical properties of soils developed on dumps originating from lignite extraction and to decipher the respective roles of the geomorphology and the presence of lignite on the biogeochemical characteristics of these soils. Soils from the Armand spoil heap, located in Peypin (Bouches-du-Rhône, France), and natural neighboring Mediterranean soils without lignite were sampled and compared. Lignite presence was assessed by ^{13}C CPMAS NMR spectroscopy allowing for the quantification of C pools such as aromatic C groups, which are characteristic signature of lignite. Physico-chemical (texture, pH, organic C, carbonate, total N, total S, CEC), mineralogical and biological (enzyme activities: β-glucosidase, arylsulfatase, acid phosphatase, arylamidase, lipase and fluorescein diacetate hydrolase; Oxitop basal respiration and Biolog® catabolic profile) parameters were analyzed in the two types of soil. Microbial activities were higher in the natural soils than in the spoil heap soils, while spoil heap samples exhibited enriched aromatic-C pools. Some variables exhibited a gradient along the slope: carbonate and sand contents were larger at the bottom of the heap while clay content, CEC, organic C and C/N ratio were larger at the top of the heap. On the contrary, microbiological activities did not follow any structured pattern according to the slope and appeared distributed as patches. Variance partitioning combined with multiple linear regressions demonstrated that the ^{13}C NMR quality of soil organic matter was the main structuring factor of microbial properties, which were in most cases reduced by the presence of lignite.

Keywords

Lignite, ^{13}C CPMAS NMR, Spoil heap, Enzymatic activities, Respirometry, CLCPs, Leptosols, Technosols

1. Introduction

Lignite, also named brown coal, is a poor-quality coal. Compared to mature coal such as anthracite, it is classified as the lowest grade coal (Van Krevelen classification) due to its high moisture content and its least carbon concentration. It has also a low heating value which explains its main use as a fossil fuel for steam-electric power generation. This fossil material can be found all around the world, with about 20 % of the reserves being located in Europe (Thielemann et al., 2007). In France, lignite was extracted in the Provence coal mine basin (south-east France) until 2003 to generate electricity in a coal-fired plant located near the pits (Meyreuil-Gardanne, France).

The mine activities were located in the sedimentary basin of the Arc, made up of old fluvio-lacustrine formations from the Upper Cretaceous with a Triassic to Jurassic basement. The Arc basin forms a 70-km-long syncline elongated from East to West (between Saint-Maximin-la-Sainte-Baume and Berre l'Etang), and 12-km-wide from North to South (between Aix-en-Provence and Marignane). The originality of the Provence mining basin is that it dates from the late Cretaceous, whereas the other French coal mining basins were formed during the Carboniferous (-359 to -299 Ma). More precisely, lignite deposits of the Provence mining basin dates from the Fuvelian, a local name corresponding to the lower Campanian (approx. 80 Ma). (Autran et al., 2014; Dheilly and Brigati, 2015; Geoderis, 2016)

The Fuvelian formation is composed of limestone (sometimes mixed with clays), clayey and/or gray lacustrine micrites, lignite layers, several levels of cement rock (i.e. a limestone containing 20-25% clay) and lateral intercalation of detrital levels with clayey or sandstone tendency. The lignite layers themselves can contain interbeds of these non-lignite substrates.

Lignite deposits were formed in a continental and lacustrine environment (i.e. a deep lake), alternately with periods of limestone sedimentation. These sedimentary characteristics were quite different from those of the carboniferous coal period (no vegetation and pedological fossilized characteristics) (Autran et al., 2014).

During its extraction, large amounts of mine overburden materials enriched in lignite were deposited near the pits, forming spoil heaps. Such dumps can cause ecosystem disturbances such as modifications in plant, animal and microbial community structures (Hüttl and Weber, 2001). However, uncapped spoil heaps of the Provence basin have been colonized by natural vegetation and pedogenetic processes have started over the past few decades, although not documented in detail (Geoderis, 2020).

Given the unique properties of lignite, many studies have investigated its influence on soil physico-chemical properties such as SOM quality, mineralogy, pH and cation exchange capacity (Rumpel et al., 2002; Shrestha and Lal, 2011; Ogala et al., 2012). Despite its central role in soil formation and nutrient recycling, far less studies have investigated the effect of lignite on the functions of soil microbial communities (Frouz and Nováková, 2005; Helingerova et al., 2010; Lehmann et al., 2011). Extracellular enzymes and Community-Level-Catabolic-Profiles (CLCPs) of soil microorganisms act as the major drivers of mineralizing and recycling functions. These parameters are known to vary concomitantly with the quality of C substrates (Alarcón-Gutiérrez et al., 2009) and may serve as indicators of SOM lability/recalcitrance and soil biological pedogenetic processes. Moreover, lignite effects on both physico-chemical and biological variables have been poorly documented under Mediterranean pedoclimatic conditions (Panagopoulos, 2013; Panagopoulos and Hatzistathis, 1995; Dixon and Schulze, 2002; Clouard et al., 2014). In fact, most of the studies dealing with lignite effects on soil properties were generally performed in low-pH environments and in typical North-European pedoclimatic conditions (e.g. the Lusatian District in Germany) (Fettweis et al., 2005). This was also emphasized in a review of Amoah-Antwi et al. (2020) which mentioned that alkaline soils remain largely untested about the effects of lignite on their pedobiological properties. Thus, there is unambiguously a gap of knowledge about the impact of lignite on soils with alkaline/calcareous properties. This lack of data is even more true if we consider the atypical nature of the lignite we studied (formed during the cretaceous period) compared to the other data available in the literature and which mostly concern lignite from carboniferous period with different physico-chemical properties.

Another gap of knowledge in literature data concerns the heterogeneity of lignite distribution in soils and its associated effects on soil properties. Indeed, to our knowledge, fine topographic assessment of the distribution of these variables on a whole spoil heap is almost never investigated, an original aspect that we aimed to investigate during our study.

Given the different gap of knowledge mentioned above, our general objective was to compare the bio-physico-chemical properties of soils developed under natural conditions (without lignite) and those of soils developed from overburden spoil heap material from a lignite mine, in Mediterranean pedoclimatic conditions characterized by a calcareous parent material, alkaline pH, sclerophyllous vegetation cover and summer drought conditions. Specific objectives were supported by two hypotheses: (i) lignite enrichment can be evidenced by the non-destructive NMR method and its presence can modulate the expression of microbial functions in soil samples; (ii) soil bio-physico-chemical properties and their interactions are influenced both by the topography of the heap and by the patchy distribution of lignite. Consequently, 4 different contour lines were sampled along the slope of the spoil heap. Near the spoil heap, 4 plots, named controls, were also sampled on the natural slope of a hill devoid of overburden material. Soil organic matter (SOM) quality was characterized by Solid-State ^{13}C Cross-Polarization Magic-Angle Spinning Nuclear Magnetic Resonance (SS ^{13}C CPMAS NMR), and pedological properties of soil samples (e.g. texture, pH, CEC, C, N, etc.) were measured. Microbial functions were assessed by CLCPs (Biolog), soil basal respiration (Oxitop) and a set of various enzymatic activities involved in the main biogeochemical CNPS cycles.

2. Materials and methods

2.1. Site description and sampling

The studied site (43°23’11.20’’N/ 5°33’28.28’’E) was located in Peypin, in south-east France, in the mine basin of Provence near Marseille. Armand’s coal heap is one of the numerous slag heaps present in the mine basin of Provence. The Armand mine shaft sinks through the different layers of limestone and lignite to a depth of 350 m. Lignite deposits form interstratified layers within the Fuvelian karstic limestone of the late Cretaceous, with an E-W average angle of dip of 8°. Only 7 layers, named “Mine” in French were exploited, 4 of them being present and exploited in all the different pitheads

129 (including the “Puits Armand”) of the coal basin. From the base of the lignite Fuvelian deposit these 4
130 layers are called “Grande Mine” (300 m deep, 2.5 – 4 m thickness), “Mauvaise Mine” (285 m deep,
131 0.7 – 1.7 m thickness), “Mine des 4 Pans” (238 m, 1.2 – 2 m thickness) and “Gros Rocher” (226 m
132 deep1 – 1.2 m thickness) (Dheilly and Brigati, 2015). Detailed stratigraphic data of the arc Basin and
133 the Armand well can be found in Espurt et al. (2012) and Monteau (2010).
134
135 The Armand mine shaft was bored between 1887 and 1890. The mine was in activity until 1954 with a
136 break between 1932 and 1941 (HBCM, 2002). Tailings were stored close to the well under the form of
137 a slag heap leaning against the hill. To this end, the tailings were dumped on the top of the slag heap
138 using tip wagons and a mechanical hauling along a chain. The structure of the slag heap was
139 constituted by a top platform and a slope. Tailings were constituted of limestone bed rock mixed with
140 lignite residues. At the end of the mining activity, the slag heap was left as it was. No other
141 management intervention/rehabilitation strategy has taken place since it was abandoned (e.g. no
142 capping layer or external inputs such as compost, soil or embankments) except for the establishment of
143 a commercial zone on the south part of the platform (between 1996 and 2007). It was not the case for
144 the north part of the platform and the slope (Fig. S1). Thus, the zone where our study was done has not
145 experienced any reworking of human origin since the cessation of the mining activity. A last point that
146 can be emphasized here concerns self-combustion. All the slag heaps of the mine basin of Provence
147 have experienced episodes of self-combustion and this was also true for the Armand slag heap (now
148 extinguished since several decades). This process results from exothermic oxydo-reduction reactions
149 between lignite and pyrite. The increase in temperature can transform the limestone into quicklime
150 then, under the action of runoff water, in slaked lime with a powdery texture, present in abundance
151 under the soil horizons (Geoderis, 2020).
152 The age of the heap was determined from the end of overburden inputs making the heap 55-y-old. The
153 heap is 45-m-high, and the mean length of its slope is about 70 m. Four topographic levels (contour
154 lines) spaced 15 m apart were studied from the foot/bottom (level 1) to the top (level 4). Within each
155 level, a systematic sampling procedure was used to collect a set of individual samples (Fig. S1).
156 Morphological descriptions of the soils classified them as Spolic Technosols (Calcic) (WRB, 2015) or

157 artificial Anthroposols (RP, 2008) composed of four horizons, namely O, AZ, AZ/Ztc (transition) and
158 Ztc horizons (Fig. S2) with a depth of up to 1 m until a pulverulent mine waste material that has
159 undergone self-combustion processes was reached. The thickness of the heap soil profiles was about
160 0.7 m on average. The samples were collected from the AZ horizon (0.10-0.20 m thickness, average
161 0.14 m) every 10 m along each topographic level. Thereafter, composite samples were performed by
162 grouping sequentially 4 to 6 contiguous individual samples along the different levels. After grouping,
163 the different composite samples were homogenized using a manual elliptical mixer. Finally, 4
164 composite samples (n = 4) were generated at each level, except for the 1st level, whose extension
165 enabled only 3 samples to be obtained (n = 3). Additionally, 4 control samples corresponding to
166 "natural" or in-place Mediterranean soils developed without any mine tailing inputs were sampled on
167 4 plots located near the spoil heap (an illustration of the sampling strategy is given in Figure S1). The
168 control soils from this natural site were Rendzic Leptosols (WRB, 2015) or Rendosols (RP, 2008) with
169 four horizons namely O, A (average thickness of 0.13 m), A/C (transition) and C horizons (Fig. S2)
170 with a maximum total depth of 0.25 m until the calcareous parental material was reached. After
171 sampling, soils were aliquoted to perform both microbial and physico-chemical analyses. A subsample
172 was air-dried at 40 °C and passed through a 2-mm sieve before physico-chemical analysis, while
173 another subsample was sieved at 2 mm and kept fresh at 4 °C before microbial analysis within a
174 month, according to the AFNOR standard NF ISO 18512.
175
176 2.2. Physico-chemical analyses
177 pH was measured in a 2.5 soil/water ratio after 2h of incubation at room temperature (pH meter WTW,
178 Germany, pJ330i/SET). Cation exchange capacity (CEC) was measured with 2.5 g soil (sieved at 2
179 mm) suspended in 50 mL of a 50 $mmol^{+}.L^{-1}$ hexaammine cobalt(III) chloride solution ($Co(NH_3)_6Cl_3$)
180 according to the method described in AFNOR NF X 31-130. The particle size analysis was done after
181 destruction of organic matter by H_2O_2, without decarbonation step, and using the sedimentation
182 technique of Robinson (pipette method) described in NF X 31-107. Total carbon was analyzed after
183 dry combustion of soil sample at 900°C and gas chromatography measurement according to NF ISO
184 10694 and total nitrogen according to NF ISO 13878. Carbonate content was determined using HCl

185 according to the gasometric method of Leo (1963). Total organic carbon (Corg) was obtained by
186 subtracting carbonate value to total carbon value. Mineralogy was characterized by X-ray diffraction
187 (XRD) performed on some soil samples, collected on both control and spoil heap plots. The protocol is
188 given in Table S1.
189
190 2.3. SS 13C CPMAS NMR spectra acquisition
191 One gram of soil was pre-treated with 45 mL of a 10 % (v/v) hydrofluoric acid solution according to
192 the modified method of Schmidt et al. (1997) before NMR analyses. The HF treatment was repeated
193 four times, followed by four rinses with distilled water. This procedure was adequate to eliminate
194 carbonate and paramagnetic compounds that may induce broadened resonances and decreased signal
195 intensities (Georgakopoulos, 2003). Following HF treatments, samples were further dried at 50 °C
196 before NMR analyses. TOC content of each soil sample was determined before and after HF treatment
197 by CHNS elemental analysis. The SS ^{13}C CPMAS NMR spectra were obtained with a Bruker Advance
198 III 400 MHz spectrometer, using a commercial two-channel, 4-mm Bruker probe head. 100 mg of air-
199 dried and ground soil sample (particle size < 0.3 mm, Cyclotec TM1093, Foss Co., France) was placed
200 in a 4-mm zirconium rotor and spun at magic-angle at 10 kHz. SS ^{13}C CPMAS NMR was performed
201 with a ramped ^{1}H pulse during a contact time of 2 msec to obtain the best signal-to-noise ratio. ^{1}H
202 decoupling was performed during the acquisition to improve the resolution. Recording 8 K transients
203 with a recycle delay of 2.5 sec represented standard conditions to obtain a good signal to-noise ratio.
204 The ^{13}C chemical shifts were referenced by tetramethylsilane (TMS) and calibrated with the glycine
205 carbonyl signal, set at 176.05 ppm. All measurements were monitored at room temperature. The
206 spectra chemical shift range of soil was characterized by the following dominant peaks: alkyl C (0–45
207 ppm), *O*-alkyl C (45–110 ppm), methoxyl C (50–60 ppm), aromatic C (110–140 ppm), phenolic C
208 (140–160 ppm) and carboxyl C (160–190 ppm). Deconvolution of the NMR spectra was performed
209 using the software DmFit (Massiot et al., 2002), and the intensity of each C region was expressed as a
210 percentage of the total C. According to Mathers et al. (2003) and Clouard et al. (2014), to obtain C-
211 quantified data (mg g^{-1}) instead of only C proportions, the percentages of each NMR spectrum region
212 were multiplied by both TOC value of residual fraction (post-HF treatment) and enrichment factor (i.e.

sample residue / sample raw mass). The degree of humification was calculated according to Baldock et al. (1997) using the alkyl-C to O-alkyl-C ratio with the respective peaks of the spectra. The ratio A was calculated according to Chabbi et al. (2007) as it follows (alkyl C + aromatic C) / (O-alkyl C + carboxyl C). The aromaticity index (AI) was calculated as AI = (A(110-160 ppm) / A(0-160 ppm)) (Lorenz et al., 2006).

2.4. Enzyme assays

The following enzyme activities, arylamidase, arylsulfatase, β-glucosidase, acid and alkaline phosphomonoesterases were measured according to the respective protocols of Tabatabai and Bremmer (1969, 1970), Eivazi and Tabatabai (1988) and Acosta-Martinez and Tabatabai (2000). The substrates used for the different enzyme assays were : 8 mM L-leucine β-naphtylamide hydrochloride (arylamidase), 5 mM *p*-nitrophenyl sulphate (arylsulfatase), 5 mM *p*-nitrophenyl-β-D-glucopyranoside (β-glucosidase), 5 mM *p*-nitrophenyl phosphate (acid and alkaline phosphomonoesterases). The buffers used for the different enzyme assays were : 0.1 M tris(hydroxymethyl)aminomethane (THAM) pH 8.0 (arylamidase), 0.5 M acetate buffer pH 5.8 (arylsulfatase), modified universal buffer (MUB) pH 6.0, MUB pH 6.5 (acid phosphomonoesterase), MUB pH 11 (alkaline phosphomonoesterase). Detailed protocols can be found in Floch et al. (2009). The method of Green et al. (2006) was modified to monitor fluorescein diacetate hydrolase activity (FDA); the pH of phosphate buffer (50 mM) used was 7.0 instead of the 7.6 as recommended by Alarcón-Gutiérrez et al. (2008b), to avoid potential non-enzymatic interferences and the substrate used was fluorescein diacetate (5 mM). Lipase, *i.e.* fluorescein dilaurate hydrolase, was measured according to the same procedure as FDA except that 5 mM fluorescein dilaurate (FDL) was used for the incubation.

For all enzyme assays, no toluene was added to the mixture because of the short incubation times. Enzyme assays were performed in 3 replicates for each soil sample (1g) at 37°C during 1 h. Control samples, i.e. without substrate added during soil incubation step, were also realized for the different enzyme assays. A unit (U) of enzyme activity was defined as μmole of substrate hydrolyzed min^{-1}, and per g of soil dry weight ($U.g^{-1}$ DW).

240

241 2.5. Basal respiration

242 Basal respiration (BR) was carried out in triplicate using the Oxitop® (WTW, Germany) system. Jars
243 fitted with CO_2 trap (NaOH pellets) were filled with soil sample (40 g) and were thereafter
244 hermetically sealed. The depression in O_2 was measured during 21 days at 20 °C in jars with the
245 automated manometric heads (Platen and Giessen-Friedberg, 2000). Basal respiration was expressed
246 in mg $O_2.g^{-1}$ DW (Alarcón-Gutiérrez et al., 2008a).

247

248 2.6. Community-Level-Catabolic-Profiles (CLCPs)

249 The Biolog® Ecoplate technique was used to characterize the CLCPs of the soil bacterial communities.
250 Briefly, 10 g of soil was added to 100 mL of a sterile sodium pyrophosphate solution (0.1 %) in a 250
251 ml flask and was shaken at 200 rpm for 20 min. The resulting mixture was 100-fold diluted with a
252 sterile NaCl solution (0.85 %). On the basis of respirometry results and according to the protocol
253 defined by Calbrix et al. (2005), dilutions were adjusted to obtain pre-defined and similar
254 concentrations of microbial cells between the different soil samples. Each dilution was used to
255 inoculate wells (31 C substrate wells + 1 control well) of the Biolog® Ecoplates (125 µL per well).
256 Plates were incubated at 25 °C and absorbance at 595 nm was measured daily for 7 days. Metabolism
257 of the different substrates in the wells resulted in the reduction of tetrazolium, which changed from
258 colorless to purple formazan. The absorbance value of the Biolog® Ecoplates control well (containing
259 no substrate) was subtracted from the absorbance of every other well, to eliminate background color
260 from the soil suspension. The average well-color development (AWCD) value was calculated from the
261 C substrate wells after 48 h of incubation (Garland and Mills, 1991). Three replicates for each soil
262 sample were performed.

263

264 2.7. Statistical analysis

265 Means and standard error of means were determined for each set of composite samples. The means
266 were compared using the Kruskal-Wallis *post hoc* test, with a significance level of $P < 0.05$.
267 Correlations between the different variables were calculated using Pearson coefficient and their

significance was tested at a level of 5%. The coefficient of variation (CV) of each variable was calculated by dividing the standard deviation by the mean (s(n)/μ). To perform ordination methods, we distinguished 3 subsets of variables in our study: the 1st subset contained the response variables (microbiological) and the 2nd and the 3rd were environmental explanatory variables, *i.e.* physico-chemical (carbonates, Corg, Ntot, C/N, clay, silt, sand, CEC) and ^{13}C NMR quality subsets respectively. Prior to multivariate analyses, a detrended correspondence analysis (DCA) was carried out using detrending by segments according to ter Braak and Smilauer (2002). Since the gradient lengths extracted were always < 1 (4 being the threshold value for a unimodal response), linear responses were expected, and thus linear ordination methods were chosen. Principal component analyses (PCA) were performed to analyze the different datasets and to show relationships between physico-chemical, ^{13}C CPMAS NMR and microbiological variables as well as to discriminate the different soil samples. Redundancy Discriminant Analyses (RDA) were performed according to the design given by Floch et al. (2009) in order to decompose the variance and to determine the relative contribution of both pedological and ^{13}C NMR quality variables on the total variance of enzyme activities. Before running RDA, collinearities were detected and variables with high variance inflation factors (VIFs > 20) were deleted. Thereafter, the remaining variables in both environmental subsets were selected using a mixed forward and backward step by step procedure with Monte Carlo permutation tests and with a k penalty parameter of 1.2. Variance partition was finally performed by running full RDA and partial RDA (pRDA) and calculated using adjusted R^2 according to Peres-Neto et al. (2006) and Borcard et al. (2011). The total variation of response model was partitioned as % of net physico-chemical and % of soil ^{13}C quality of explained variance. The statistical significance of the different fractions was tested with Monte Carlo permutation tests ($\alpha = 0.001$). Multiple linear regression (MLR) was also performed on each individual microbial variable and its selected subsets of environmental explicative variables. Adjusted-R^2 and β-coefficients of each MLR model were calculated and tested at $P < 0.05$. Statistical analyses were performed using CANOCO version 4.5 (Biometris, The Netherlands) and XLSTAT (Addinsoft, 2011 version, UK) software and both ADE4 and Vegan packages of the R project for statistical computing.

296

297 **3. Results**

298 We distinguished 3 subsets of variables: physico-chemical (carbonates, Corg, Ntot, C/N, clay, silt,
299 sand, CEC, pH), ^{13}C NMR markers of C quality, and microbiological variables. It appeared that for
300 most of them their coefficients of variation (CV), i.e. their dispersion, were high, which made some
301 differences non-significant between the spoil heap levels and/or the controls from the neighboring
302 natural site (Fig. S3). Total organic carbon (CV=0.38), aromatic C contents (CV=0.46), and lipase
303 activity (FDL; CV=0.66)) showed the highest coefficient of variation for physico-chemical, NMR and
304 microbiological variables respectively. To reduce the dimensionality of the data, several ordination
305 methods were carried out on the different soil samples (PCA, DCA and RDA).

306

307 3.1. Soil physico-chemical and ^{13}C NMR characteristics

308 Results of the soil physico-chemical analyses are given in Table 1. Several physico-chemical
309 characteristics differed significantly between control soils of the natural site and spoil heap soils.
310 Control soils showed significant higher clay content (342 g kg^{-1} on average) than soils from the slope
311 of the slag heap (ranging on average between 135 and 175 g kg^{-1}). On the contrary, sand content in
312 control soils (222 g kg^{-1} on average) was significantly lower than those of the slag heap (ranging on
313 average between 387 and 520 g kg^{-1}). According to the USDA soil textural classification, soils from
314 the coal heap were thus mainly loam soils, while control soils were mainly clay loam soils (Fig. S4).
315 Carbonate content showed the lowest average value in control soils (400 g kg^{-1} on average), which was
316 significantly lower than carbonate contents of soils from the top (Level 4, 461 g kg^{-1} on average) and
317 the foot (Level 1, 656 g kg^{-1} on average) of the slag heap. CEC of control soils (25 $cmol^{+}$ kg^{-1} on
318 average) showed significant difference, but only with soils from the foot of the slag heap (39.1 $cmol^{+}$
319 kg^{-1} on average). Mineralogy differed between control soils and coal heap soils. Detailed results are
320 given in Table S1. Briefly, calcite, illite, muscovite and quartz were present in all samples. Hematite
321 and anorthite were only present in coal heap soils. On the contrary dolomite and clinochlore were only
322 present in the control soils.

323

Considering only the soil samples of the slope of the spoil heap, some physico-chemical variables were structured according to an altitudinal gradient. The carbonate (656 > 524 / 562 > 461 g kg^{-1}) and sand contents (520 > 442 > 436 > 387 g kg^{-1}) decreased with increasing altitude level (from level 1 to level 4), while the inverse pattern was observed for Corg (5.1 < 8 < 9.7 < 11.3 %), C/N (10.1 < 14 < 14.1 < 19.7), clay (135 < 169 / 166 < 175 g kg^{-1}) and silt contents (346 < 389 < 395 < 439 g kg^{-1}) and CEC (25 < 34.2 < 37.1 < 40.4 $cmol^{+}$ kg^{-1}). These trends were more evident following principal component analysis (PCA) (Fig. 1), which highlighted, except for samples from the level 2, a gradual distribution of heap samples (levels 1, 3 and 4) along the 1st axis defined by these variables.

In complement, the quality of organic carbon was assessed using SS ^{13}C CPMAS NMR (Tab. 2) and a PCA was also performed to discriminate samples according to their C quality (Fig. 2). Phenolic C and methoxyl C were the sole fractions to show no significant differences between samples, whether they came from the slag heap or from the control plot. Aromatic C, ratio A and aromatic index (AI) were significantly lower in control samples than in the spoil heap samples (respectively up to 3.3, 3.1 and 3 times lower), except for those of level 1, making it possible to discriminate them from heap samples on the PCA factorial map (Fig. 2). The opposite pattern was observed for *O*-Alkyl-*C* which was a fraction significantly more abundant in control soils than in all the slag heap soils (up to 2.5 times higher). The distribution of the other C signals between control and spoil heap samples was clearly heterogeneous. When considering only the samples of the heap slope, level 1, which corresponded to the foot of the spoil heap, had systematically the lowest contents in the different C fractions, while a gradual decrease was observed for some of the C signals from level 4 to level 1. This was perceptible on the 1st PCA map (Fig. 2) for recalcitrant C, such as aromatic C content, and ratios A and AI.

3.2. Soil microbiological variables

Results of the microbiological variables are given in the Table 3. β-glucosidase activity was significantly higher in controls (6.95 mU g^{-1} MS on average) than in most of the spoil heap samples (ranging on average between 4.7 and 5 mU g^{-1} MS). However, activity of the control soils was not significantly different from those of the heap foot (Level 1, 5.7 mU g^{-1} MS on average). The acid

352 phosphatase activities were significantly 2.5 to 2.8 times higher in the control soils (170.7 mU g^{-1} MS)
353 than in the soil samples from the different levels of the slag heap (ranging on average between 61.2
354 and 67.4 mU g^{-1} MS). No significant differences in acid phosphatase activities were observed between
355 the soils of the different spoil heap levels. The arylsulfatase activities were significantly 4.2 to 5 times
356 higher in the control soils (368.7 mU g^{-1} MS on average) than in the soil samples from the different
357 levels of the slag heap (ranging on average between 74.3 and 88 mU g^{-1} MS). As also observed for the
358 acid phosphatase and the β-glucosidase activities, no significant differences in the arylsulfatase
359 activities were observed between the soils of the different spoil heap levels. No significant differences
360 in respiration activities were observed between the control and the spoil heap samples. However, a
361 gradient of respiratory activity was observed between soil samples along the slope of the slag heap
362 with significant differences between the levels 1-2 (1.79 and 1.75 mg O_2 g^{-1} d^{-1} on average) and the
363 level 4 (3 mg O_2 g^{-1} d^{-1} on average). No significant differences between the different samples (i.e. spoil
364 heap levels and controls) were observed for alkaline phosphatases, arylamidases, FDA and lipases
365 (FDL) activities. Finally, AWCD of the different samples was not significantly different between the
366 spoil heap and the control soils, thus indicating similar CLCPs in both the spoil heap levels and the
367 controls.
368 On a multivariate basis, PCA revealed that controls were clustered at the positive end of the 1st axis
369 and thus were well discriminated from spoil heap samples (Fig.3), indicating that control soils were
370 biologically the most active. In the case of the spoil heap samples it was not possible to discern any
371 multivariate pattern structured according to elevation because of the patchy distribution of the different
372 activities along the slope.
373
374 3.3. Correlations and variance partition
375 The detailed examination of univariate Pearson correlation coefficient between the different variables
376 indicated some significant correlations (Tab. 4), the highest negative correlation detected being the one
377 between FDA and ratio A (-0.71).
378 Partitioning of the variance in the response data (microbiological) into the contribution of the two
379 subsets of environmental variables (*i.e.* physico-chemical and ^{13}C NMR quality) was thereafter

performed on the whole (heap and controls) and the reduced (heap only) datasets (Fig. 4) as well as on each distinct response variable (heap only).

Prior to partitioning, the most significant variables in the two subsets of environmental variables were selected using a step by step procedure and RDA. This selection is given in supplementary data (Table S2). Thereafter, the selected variables were also used to perform multiple linear regressions (Tab.5).

For both the whole and reduced datasets (i.e. control + spoil heap samples; spoil heap samples only), the sum of the net (marginal) explained variances (i.e. physico-chemical and ^{13}C NMR) was twice higher considering only the spoil heap model (44 % vs 23 %) (Fig. 4). For both datasets, explained net variance of NMR variables was twice higher than that of physico-chemical variables (26.5 % vs 13.2 %). Explained variance of each microbiological variable was performed only on soil heap samples (Fig. 4). Strong variations of total net explained variances were observed as a function of the microbial variable considered. Arylsulfatase, alkaline phosphatase and arylamidase activities showed the highest explained variances (between 89 and 69 %) whereas AWCD (Biolog) and FDA had the lowest values (5.2 and 6.7 % respectively). Partitioning the variance between physico-chemistry and ^{13}C NMR effects on microbiological variables also showed large differences. For some microbial variables, variances were more explained by net effects of ^{13}C NMR variables (arylamidase 98 %, β-glucosidase 96 %, lipase (FDL) 83 %, respiration 77 %, FDA 73 %), while the variances of other microbiological variables were more explained by net effects of physico-chemical variables (acid phosphatase 85 %, arylsulfatase 67 %, alkaline phosphatase 64 %). From the environmental variables previously selected by RDA (Tab. S2), multiple linear regression analyses (MLR) were also generated for each microbial variable. Significant adjusted R^2 and β-coefficients are given in Table 5. The highest and significant R^2 were obtained with the ^{13}C NMR quality. Moreover, β-coefficients were calculated and were complementary to the previous statistical calculations, enabling negative or positive effects of the different explicative variables to be visualized. The most significant effects were negative NMR effects which were mainly attributed to recalcitrant C, *i.e.* aromatic, phenolic and alkyl C contents. Accordingly, the best models were obtained for arylamidase (adj. R^2 0.86***) and β-glucosidase (adj.

R^2 0.59**) activities, which were clearly and negatively influenced by the richness in aromatic C. Three other microbial variables, FDL, FDA and basal respiration, were less strongly but significantly influenced by C quality signature (adj. R^2 of 0.35*, 0.44* and 0.47* respectively), especially the content in alkyl-C. Some significant models were also obtained between some microbial variables (β-glucosidase, arylsulfatase, FDA, Oxitop BR) and physico-chemical variables (carbonate, N, clays, CEC), but their levels of significance were lower than those obtained with the sub-set of NMR variables (adj. R^2 ranging between 0.23* and 0.41*).

4. Discussion

Lignite or coal waste tailings have considerably modified large surface areas worldwide. This is also the case in the Provence coal mine basin, in France. Currently, only a few deposits remain visible at a landscape scale because of their natural spontaneous plant colonization. Concomitantly to the establishment of the vegetation, soils have developed on the tailings. Our objectives were to characterize these soils and to compare their properties to those developed on the neighboring natural substratum, and in particular, to decipher the role of both the geomorphology and the presence of lignite in the spatial structuring of the biogeochemical characteristics of these soils. It was not possible to directly quantify the total amount of lignite remaining in the different soil profiles, as the quantification of lignite in soils or mine coal wastes remains a challenge (Roth et al., 2012). Characterization of the organic matter quality by solid state ^{13}C NMR was thus necessary to track the presence of lignite in the surface horizons. This proxy was tested and validated by Clouard et al. (2014) and Rumpel et al. (1998), who showed that aromatic C, aromatic index and ratio A parameters were typical of the presence of lignite in soil.

4.1. Spoil heap soils significantly differ from control soils

We first aimed to compare the typology of control soils from the natural site and heap soils measuring both physico-chemical and microbiological variables. Control and spoil heap soils presented the same sequence of poorly developed horizons, but their morphology and their physico-chemical characteristics were different as detailed below.

435 The main morphological difference between the two types of soil was the thickness of the whole soil
436 profile: while control soils presented a maximum of 0.25 m thickness, the average thickness of the
437 heap soils was about 0.7 m (Fig. S2). This larger thickness may be due to the loose/powdery material
438 characteristic in which the heap soils develop allowing for an accelerated water circulation and thus
439 pedogenesis in the chore of the material unlike for the control soils, which are developed from hard
440 limestone. Some physico-chemical properties also differed between control and coal heap soils.
441 Controls were clearly richer in clay and on the contrary poorer in sand indicating a clay loam texture,
442 while coal heap soils were exclusively classified as loam. The texture, added to soil thickness,
443 indicated that spoil heap possessed physically favorable characteristics for vegetation establishment as
444 observed on site where both control and spoil heap stands were visually very similar. In addition, the
445 thickness of the A horizon was similar on both the spoil heap and in the control soils after only 55
446 years, indicating an active early pedogenesis or a reduced organic matter mineralisation due to lower
447 enzymatic activities and leading to an enhanced stock of organic matter. However, the extent of the
448 organo-mineral aggregation and its stability would need further study to conclude on the physical
449 fertility status of these soils. A related and interesting study was performed by Panagopoulos and
450 Hatzistathis (1995) on spoil heaps from lignite mining in Greece, under the same bioclimatic
451 conditions (*i.e.* sub-humid Mediterranean bioclimate) and on a similar mineral substratum (*i.e.*
452 calcareous). On their naturally revegetated stands, the texture of the A horizons was similar (145-200 g
453 kg^{-1} clay, 340-460 g kg^{-1} silt and 180-230 g kg^{-1} sand) to that of the Armand soils. In addition, in a
454 previous study (Clouard et al., 2014), we compared an aged soil developed on a lignite outcrop of the
455 same origin as the lignite exploited at the Armand mine, and a nearby natural soil without lignite,
456 similar to the Armand control soils. Control soils (without lignite) of these two sites had similar
457 textures (clay loam / silty clay loam, (Fig. S4), a similarity which can be explained by both the same
458 geological parent material and the same Mediterranean vegetation cover (scrubland dominated by
459 *Quercus alba* and *Pinus Halepensis*). On the contrary, when comparing soils from these two studies
460 developed in the presence of lignite, differences in texture were observed between spoil heap and
461 outcrop soils. Aged soil (geological) had a finer texture (silty clay) than young soils (spoil heap),
462 which presented a loamy texture. This comparison suggests that, on the long term, the presence of

463 lignite, in combination with bedrock limestone, may affect soil texture and thus soil physico-chemical
464 quality. However, we are aware that care must be taken with this hypothesis because Clouard et al.
465 (2014) investigated natural soils whereas our present study was done on technosols with complex
466 historical traits of life.
467 Considering C contents, with mean values of respectively 550 g kg^{-1} and 85 g kg^{-1}, carbonate and Corg
468 contents of the Armand spoil heap soils were also similar to those reported by Panagopoulos and
469 Hatzistathis (1995) (553 g kg^{-1} and 73.7 g kg^{-1} respectively). Therefore, for these physico-chemical
470 variables, it seems that the dynamics patterns observed could represent a general trend for unmanaged
471 young spoil heap soils under similar mineral parent material and bioclimatic conditions. However, in
472 the case of N_{tot} content and C/N values, our results diverged from those of Panagopoulos (2013), since
473 we obtained higher N_{tot} values and therefore lower C/N ratios. This can be easily explained by the age
474 of the spoil heaps, the plant colonization chronosequence and the establishment of soil N_2 fixing
475 microbial communities as mentioned by Baldrian et al. (2008) on brown coal heap. Indeed, the
476 Armand spoil was 55 years old, while the spoils described by Panagopoulos (2013) were only 14 years
477 old. Moreover, this may reflect a more evolved soil organic matter status since N and C/N values were
478 close to those of the nearby control soils. Heap soils also exhibited some differences in their
479 mineralogical composition. Unlike in the control plots, dolomite and clinochlore were absent in the
480 spoil heap soils, whereas hematite and anorthite were only present in spoil heap soils. Anorthite is
481 highly weatherable and it may favor an early pedogenesis. Lignite is known to contain
482 pyrite/marcasite (FeS_2) (Ogala et al., 2012) , which oxidation can induce the formation of hematite and
483 thus explain its presence in the spoil heap. Alternatively, hematite could be either inherited from the
484 calcareous rock or the result of combustion processes (Masalehdani et al., 2009) that occur in spoil
485 heaps with lignite or coal residues (Thiery et al., 2013); as already mentioned, self-combustion is
486 indeed an event that occurred in the past on the Armand spoil heap before its spontaneous plant
487 colonization.

Microbial analyses showed that control soils had globally higher microbial activities than heap soils, with acid phosphatase, arylsulfatase and β-glucosidase activities being the best differentiating variables. ^{13}C CPMAS NMR analysis also discriminated between control and spoil heap soils. Control soils had higher contents in O-Alk-C than spoil heap soils, which were richer in structures more recalcitrant to C biodegradation such as aromatic C. Soil organic matter (SOM) quality between control and heap soils was clearly and significantly different, and this parameter has been recognized (Alarcon-Gutierrez et al., 2009) to influence microbial biomass and microbial activities (e.g. enzyme activities). Thus, the richness in easily assimilable C contents (O-Alk-C including carbohydrates) was probably the main driver explaining the higher enzyme activities observed in the control soils.

4.2. Variable evolution along the slope of the spoil heap

One objective of our study was to test the role of the slope as a discriminating factor for soil characteristics. We thus spatialized soil-bio-physico-chemical properties along the slope and investigated the determinism of their interactions. Some physico-chemical properties did indeed present a gradient along the slope. The foot of the spoil heap was characterized by enrichment in sand and carbonate, while the highest values in clay, CEC, Corg contents and C/N were observed at the highest levels. The most probable explanation for this trend is that the calcareous sand (probably present in the dumped material), having no cohesion and being more sensitive to erosion, tended to accumulate downhill during rainy events at the early stage of dumping, while no vegetation had yet been established. There is no obvious on-going erosion, which is now prevented by the actual dense vegetation. No dissolution and/or precipitation figures were observed in the soil profiles that would support a soluble transport. This agrees with Nyssen and Vermeersch (2010), who found that slope affects the geomorphic dynamic, the coarse elements being more abundant at the foot of a spoil. The resulting larger clay content at the top of the heap may have helped stabilize organic matter and therefore induce an increase in CEC and Corg. This may also explain the gradients in the ^{13}C NMR quality observed for some C pools: aromatic C and alkyl C were far more abundant at the top of the heap probably because of the larger clay and Corg contents.

Despite these trends, many parameters presented high coefficients of variation, thus also revealing a patchy co-structure. A similar kind of heterogeneous spatial distribution was also observed by Frouz et al. (2011), who argued that this heterogeneity is determined by many biotic and abiotic factors, as well as their interactions. This is especially true for spoil anthropogenic soil characterized by their traits of life and the heterogeneity of the deposited material itself and the way it was dumped (Baldrian et al., 2008) which, as a result, can induce a heterogeneous vegetation development and concomitant spatially heterogeneous pedogenetic processes (Boruvka et al., 2012). The age of the pines was determined along the slope and did not show any structured pattern according to the position of the trees on the slope, and thus belongs to such a paradigm (Dr F. Guibal, personal communication). For the last subset of variables, *i.e.* microbial activities, neither gradient, nor any structured pattern were observed. These response variables had a patchy distribution that calls for other explanations which are discussed below.

4.3. Lignite impacts SOM quality and microbial activities

Spoil heap samples were clearly enriched in aromatic C and thus had high AI and ratio A values, which are typical of a lignite signature (Chabbi et al., 2007; He et al., 2019). These results confirmed our previous results obtained with a soil developed from a lignite outcrop (Clouard et al., 2014). They are also in accordance with several other studies performed on various soils enriched in lignite and mentioning high peaks in the aromatic C region (Kögel-Knabner, 1997; Rumpel et al., 1998; Kögel-Knabner, 2000; Rumpel et al., 2000 a & b; Fettweis et al., 2005). The higher values of these proxies were concomitant with a decrease in microbial activities. From diverse ordination techniques, our results clearly evidenced that microbial activities of the spoil heap were mainly structured by the quality of SOM in relation with the presence of lignite, with lignite abundance indicators having negative effects on most of the microbial variables. Up to now, an explanation for this phenomenon has remained difficult to establish. Lignite has been suggested to be an inert material and very few studies have mentioned the possibility for microorganisms to use it as a C source (Opara et al., 2012). Rumpel et al. (2001) and Rumpel and Kogel-Knabner (2004) mentioned the possibility for soil

543 microorganisms to transform and incorporate lignite in their biomass, but the C proportion was very
544 low compared to recent soil organic matter. Considering potential effects on the composition of soil
545 microbial communities, Tran et al. (2015) reported that lignite had very limited impacts on soil
546 microbial biodiversity. In our study, we suggest that the lower microbial activities observed in the
547 spoil may be due to a relative enrichment in the C pool derived from lignite (black carbon), which is
548 more recalcitrant to degradation by microorganisms and thus limits the expression of their
549 mineralizing enzymes. We observed the same activity pattern (Clouard et al., 2014) in a soil developed
550 from a lignite outcrop. In that study, the use of a Δ 14C model (Stuiver and Polach, 1977; Rumpel et
551 al., 2003) allowed us to distinguish the functional relationships between microorganisms and the two
552 C pools, i.e. fossil black C and recent plant C. It demonstrated that the recent C pool was the sole C
553 fraction able to exert a positive influence on microbial activities, while the black C pool was devoid of
554 any stimulating effect on soil microbial metabolism. Unfortunately, C ranges between our 2 studies
555 were very different, ruling out the extrapolation to the Armand spoil of the model we used for the
556 lignite outcrop to quantify both recent and lignite C pools, probably because of the large difference in
557 soil age. Another explanation may be a direct inhibitive effect of lignite, especially on enzyme
558 activity, as it has been shown that charcoal can adsorb enzymes and can thus reduce their activities
559 (Daoud et al., 2010; Wang et al., 2011).
560
561 **5. Conclusions**
562
563 This study was performed because of the gap of knowledge about lignite effects on characteristics and
564 functioning of calcareous/alkaline soils. The approach chosen was to consider the topography of the
565 slag heap and to demonstrate : i) that soil properties were heterogeneously distributed or influenced by
566 the slope of the slag heap and ii) that lignite presence could modulate the expression of microbial
567 functions.
568 Control soils from the natural site and spoil heap soils differed in their ^{13}C NMR signature with
569 aromatic C, ratio A and aromatic index (AI), typical of lignite and, which were higher in spoil heap
570 soils. They also differed in their microbiological activities, which were higher in control soils. The

lower activities observed in the spoil soils may be due to a relative enrichment in the C pool derived from lignite. The presence of lignite also discriminated soils from the heap: the patchy distribution of lignite on the heap induced a patchy distribution of microbial activities.

Heap soils were also discriminated according to their location along the slope: soils at the top of the heap had higher clay and lower carbonate contents, while soils at the bottom of the spoil heap had higher CEC, carbonate and sand contents. This trend highlights the importance of physical evolution of the heap, probably during the early stage of soil development, when vegetation is scarce. Also, control and heap soils differed in texture, with more clay in control soils than in heap soils, which can be explained by the different "parent" materials and duration of the pedogenesis processes of the two pedosystems.

This study also evidenced a very active pedogenesis since thick soil profiles developed on the spoil heap in a few decades (within 55 years). As we mentioned in the site description section (see 2.1.), the formation of slaked lime with a powdery texture following past events of self-combustion of the spoil heap is also probably of major importance for explaining the quickness of soil formation. This confirms the interest of studying lignite mine tailings in a context of calcareous/alkaline soils because, under acidic conditions, soil formation is recognized in the literature to be slower with the need of remediation procedures.

In conclusion, the pedogenesis of soils on lignite spoil heaps seems to be quite rapid and the evolution trend depends on the heap morphology and the presence of lignite, which has either a negative or at least no effect on microbiological activities. As they gradually blend into the landscape, the slag heaps become less and less easily identifiable, especially the oldest heaps such as the Armand heap. Nevertheless, after only 55 years, age of the Armand slag heap, we can consider that the soils are still in phase of evolution and that it is difficult to predict what their future evolution will be. It would therefore be desirable to monitor these heaps over the long term in order to contribute to a better understanding of this specific anthropogenic environment and to obtain data that would be useful for mine site remediation.

Acknowledgements

This work was supported by the Human-Environment Observatories of the Mine basin of Provence and the French National Center for Scientific Research (CNRS-INEE). We thank Samuel Robert (CNRS-ESPACE, France) for haring his knowledge of the context of the mine basin of Provence, which led us to study the Armand site. We wish to thank Mr. Virgile Calvert for helping on soil sampling.

608 **References**

609 Acosta-Martinez, V., Tabatabai, M.A., 2000. Arylamidase activity of soils. Soil Sci. Soc. Am. J. 64,
610 215-221.
611
612 Alarcón-Gutiérrez, E., Couchaud, B., Augur, C., Calvert, V., Criquet, S., 2008a. Effects of nitrogen
613 availability on microbial activities, densities and functional diversities involved in the degradation of a
614 Mediterranean evergreen oak litter (*Quercus ilex L.*). Soil Biol. Biochem. 40, 1654-1661.
615
616 Alarcón-Gutiérrez, E., Floch, C., Augur, C., Le Petit, J., Ziarelli, F., Criquet, S., 2009. Spatial
617 variations of chemical composition, microbial functional diversity, and enzyme activities in a
618 Mediterranean litter (*Quercus ilex L.*) profile. Pedobiologia 52, 387-399.
619
620 Alarcón-Gutiérrez, E., Floch, C., Ruaudel, F., Criquet, S., 2008b. Non-enzymatic hydrolysis of
621 fluorescein diacetate (FDA) in a Mediterranean oak (*Quercus ilex L.*) litter. Eur. J. Soil Sci. 59, 139-
622 146.
623
624 Autran, J., Lochard, T., Monteau, R., 2014. L'exploitation dans le bassin minier de Provence :
625 quartiers, puits et galeries. Aix-en-Provence, CNRS – OHM bassin Minier de Provence, TOHM, 2, 88
626 pages.
627
628 Baldock, J.A., Oades, J.M., Nelson, P.N., Skene, T.M., Golchin, A., Clarke, P., 1997. Assessing the
629 extent of decomposition of natural organic materials using solid-state ^{13}C NMR spectroscopy. Aus. J.
630 Soil Res. 35, 1061-1083.
631
632 Baldrian, P., Trogl, J., Frouz, J., Snajdr, J., Valaskova, V., Merhautova, V., Cajthaml, T., Herinkova,
633 J., 2008. Enzyme activities and microbial biomass in topsoil layer during spontaneous succession in
634 spoil heaps after brown coal mining. Soil Biol. Biochem. 40, 2107-2115.
635

636 Borcard, D., Gillet, F., Legendre, P., 2011. Numerical Ecology with R, Springer, New York, 306 p.
637
638 Boruvka, L., Kozak, J., Muehlhanselova, M., Donatova, H., Nikodem, A., Nemecek, K., Drabek, O.,
639 2012. Effect of covering with natural topsoil as a reclamation measure on brown-coal mining
640 dumpsites. J. Geochem. Explor. 113, 118-123.
641
642 Calbrix, R., Laval, K., Barray, S., 2005. Analysis of the potential functional diversity of the bacterial
643 community in soil: a reproducible procedure using sole-carbon-source utilization profiles. Eur. J. Soil
644 Biol. 41, 11-20.
645
646 Chabbi, A., Rumpel, C., Kögel-Knabner, I., 2007. Stable carbon isotope signature and chemical
647 composition of organic matter in lignite-containing mine soils and sediments are closely linked. Org.
648 Geochem. 38, 835-844.
649
650 Clouard, M., Criquet, S., Borschneck, D., Ziarelli, F., Marzaioli, F., Balesdent, J., Keller, C., 2014.
651 Impact of lignite on pedogenetic processes and microbial functions in Mediterranean soils. Geoderma
652 232, 257-269.
653
654 Daoud, F.B.O., Kaddour, S., Sadoun, T., 2010. Adsorption of cellulase Aspergillus niger on a
655 commercial activated carbon: Kinetics and equilibrium studies. Colloid Surface B 75, 93-99.
656
657 Dheilly, A., Brigati, B., 2015. Gestion du réservoir minier de Gardanne, Bouches du Rhône :
658 Approches environnementales et hydrauliques du pompage et de son rejet dans la Mer Méditerranée ;
659 Exploitations minières passées et présentes : Impacts environnementaux et sociétaux, 17, pp. 71-84,
660 Collection EDYTEM. hal-01100951.
661
662 Dixon, J.B., Schulze, D.G., 2002. Soil mineralogy with environnemental applications, SSSA Book
663 series 7, Madison, wisconsin, USA, 866 p.

664

665 Eivazi, F., Tabatabai, M.A., 1988. Glucosidases and galactosidases in soils. Soil Biol. Biochem. 20,
666 601-606.

667

668 Espurt, N., Hippolyte, J.-C., Saillard, M., Bellier, O., 2012. Geometry and kinematic evolution of a
669 long-living foreland structure inferred from field data and cross section balancing, the Sainte-Victoire
670 System, Provence, France. Tectonics 31, TC4021, doi:10.1029/2011TC002988.

671

672 Fettweis, U., Bens, O., Hüttl, R.F., 2005. Accumulation and properties of soil organic carbon at
673 reclaimed sites in the Lusatian lignite mining district afforested with *Pinus sp*. Geoderma 129, 81-91.

674

675 Floch, C., Capowiez, Y., Criquet, S., 2009. Enzyme activities in apple orchard agroecosystems: How
676 are they affected by management strategy and soil properties? Soil Biol. Biochem. 41, 61-68.

677

678 Frouz, J., Kalčík, J., Velichová, V., 2011. Factors causing spatial heterogeneity in soil properties, plant
679 cover, and soil fauna in a non-reclaimed post-mining site. Ecol. Eng. 37, 1910-1913.

680

681 Frouz, J., Nováková, A., 2005. Development of soil microbial properties in topsoil layer during
682 spontaneous succession in heaps after brown coal mining in relation to humus microstructure
683 development. Geoderma 129, 54-64.

684

685 Garland, J.L., Mills, A.L., 1991. Classification and characterization of heteroptrophic microbial
686 communities on the basis of patterns of community level sole-carbon-source utilization. Appl.
687 Environ. Microb. 57, 2351-2359.

688

689 Geoderis, 2016. Bassin de lignite de Provence (13). Révision et mise à jour des aléas liés à l'ancienne
690 activité minière. Rapport de Synthèse. Rapport S 2016/004DE – 16PAC22070. [WWW Document].

691 URL (last accessed 23/07/06). https://www.bouches-du-
692 rhone.gouv.fr/content/download/34133/195732/file/S2016-004DE.pdf
693
694 Geoderis, 2020. Bassin lignitifère de Provence. Révision des aléas échauffement, tassement et
695 glissement sur les dépôts liés à l'exploitation minière sur les communes de Cadolive, Fuveau, Peypin
696 et Saint-Savournin. Rapport 2020/171DE – 20PAC3602. [WWW Document]. URL (last accessed
697 23/07/06). https://www.mairiedefuveau.fr/wp-content/uploads/2022/06/2020-171DE.pdf
698
699 Georgakopoulos, A., 2003. Aspects of solid state ^{13}C CPMAS NMR spectrosocopy in coals from the
700 Balkan peninsula. J. Serb. Chem. Soc. 68, 599-605.
701
702 Green, V.S., Stott, D.E., Diack, M., 2006. Assay for fluorescein diacetate hydrolytic activity:
703 Optimization for soil samples. Soil Biol. Biochem. 38, 693-701.
704
705 HBCM, 2002. Ensemble des 12 concessions du bassin de Provence. Saint-Etienne (42000). Houillères
706 de Bassin du Centre et du Midi - Direction des Sites Arrêtés 1, 95.
707
708 He, Q., Yeasmin, H., Hoadley, A., Qi, Y., 2019. Physical and chemical changes in lignite during
709 mechanical and thermal dewatering process and associated changes in the organic compounds in
710 wastewater. Int. J. Coal Prep. Util. DOI : 10.1080/19392699.2019.1682563
711
712 Helingerova, M., Frouz, J., Santruckova, H., 2010. Microbial activity in reclaimed and unreclaimed
713 post-mining sites near Sokolov (Czech Republic). Ecol. Eng. 36, 768-776.
714
715 Hüttl, R.F., Weber, E., 2001. Forest ecosystem development in post-mining landscapes : a case study
716 of the Lusatian lignite district. Naturwissenschaften 88, 322-329.
717

718 Kögel-Knaber, I., 1997. ^{13}C and ^{15}N NMR spectroscopy as a tool in soil organic matter studies.
719 Geoderma 80, 243-270.
720
721 Kögel-Knabner, I., 2000. Analytical approaches for characterizing soil organic matter. Org. Geochem.
722 31, 609-625.
723
724 Lehmann, J., Rillig, M.C., Thies, J., Masiello, C.A., Hockaday, W.C., Crowley, D., 2011. Biochar
725 effects on soil biota – A review. Soil Biol. Biochem. 43, 1812-1836.
726
727 Leo, M.W.M., 1963. Soil lime measurement, Determination of soil carbonates by a rapid gasometric
728 method. J. Agr. Food Chem. 11, 452-455.
729
730 Lorenz, K., Preston, C.M., Kandeler, E., 2006. Soil organic matter in urban soils: Estimation of
731 elemental carbon by thermal oxidation and characterization of organic matter by solid-state ^{13}C
732 nuclear magnetic resonance (NMR) spectroscopy. Geoderma 130, 312-323.
733
734 Masalehdani, N.N., Mees, F., Dubois, M., Coquinot, Y., Potdevin, J.L., Fialin, M., Blanc-Valleron,
735 M.M., 2009. Condensate minerals from a burning coal-waste heap in Avion, Northern France. Can.
736 Mineral. 47, 573-591.
737
738 Massiot, D., Fayon, F., Capron, M., King, I., Le Calve, S., Alonso, B., Durand, J.O., Bujoli, B., Gan,
739 Z.H., Hoatson, G., 2002. Modelling one- and two-dimensional solid-state NMR spectra. Magn. Reson.
740 Chem. 40, 70-76.
741
742 Mathers, N.J., Xu, Z., Blumfield T.J., Berners-Price, S.J., Saffigna, P.G., 2003. Composition and and
743 quality of harvest residues and soil organic matter under windrow residue management in youg hoop
744 pine plantations as revealed by solid-state ^{13}C NMR spectroscopy. Forest Ecol. Manag. 175, 467-488.
745

746 Monteau, R., 2010. Le lignite du Bassin de l'Arc (Bouches du Rhône). A.P.B.G. 2-06-2010. [WWW
747 Document]. URL (last accessed 23/07/06). https://www.pedagogie.ac-aix-
748 marseille.fr/upload/docs/application/pdf/2011-09/le_lignite_du_bassin_de_l_arc_apbg.pdf
749
750 Nyssen, J., Vermeersch, D., 2010. Slope aspect affects geomorphic dynamics of coal mining spoil
751 heaps in Belgium. Geomorphology 123, 109-121.
752
753 Ogala, J., Siavalas, G., Christanis, K., 2012. Coal petrography, mineralogy and geochemistry of lignite
754 samples from the Ogwashi–Asaba Formation, Nigeria. J. Afr. Earth Sci. 66–67, 35-45.
755
756 Opara, A., Adams, D.J., Free, M.L., McLennan, J., Hamilton, J., 2012. Microbial production of
757 methane and carbon dioxide from lignite, bituminous coal, and coal waste materials. Int. J. Coal Geol.
758 96-97, 1-8.
759
760 Panagopoulos, T. (2013). Factors of Reclamation Success at the Lignite Strip-mined Land in Northern
761 Greece. Journal of Tourism, Sustainability and Well-Being, 1 (2), 96-122.
762
763 Panagopoulos, T., Hatzistathis, A., 1995. Early growth of *Pinus nigra* and *Robinia pseudoacacia*
764 stands : contribution to soil genesis and landscape improvement on lignite spoil in Ptolemaida.
765 Landscape Urban. Plan. 32, 19-29.
766
767 Peres-Neto, P.R., Legendre, P., Dray, S., Borcard, D., 2006. Variation partitionning of species data
768 matrices: estimation and comparison of fractions. Ecology 87, 2614-2625.
769
770 Platen, H., Giessen-Friedberg, F., 2000. Validation of the OxiTop measuring system for the
771 determination of respiratory activity in soils and other solids. 1st Symposium on "Biological
772 degradability" 1, 13.
773

774 Roth, P.J., Lehndorff, E., Brodowski, S., Bornemann, L., Sanchez-Garcia, L., Gustafsson, O.,
775 Amelung, W., 2012. Differentiation of charcoal, soot and diagenetic carbon in soil : Method
776 comparison and perspectives. Org. Geochem. 46, 66-75.
777
778 RP, 2008. Référentiel pédologique. Baize, D., Girard, M.C. (Eds.). Editions Quae, 2009, Versailles,
779 France.
780
781 Rumpel, C., Balesdent, J., Grootes, P., Weber, E., Kogel-Knabner, I., 2003. Quantification of lignite-
782 and vegetation-derived soil carbon using 14C activity measurements in a forest chronosequence.
783 Geoderma 112, 155-166.
784
785 Rumpel, C., Grootes, P.M., Kogel-Knabner, I., 2001. Characterisation of the microbial biomass in
786 lignite-containing mine soils by radiocarbon measurements. Soil Biol. Biochem. 33, 2019-2021.
787
788 Rumpel, C., Knicker, H., Kögel-Knaber, I., Skjemstad, J.O., Hüttl, R.F., 1998. Types and chemical
789 composition of organic matter in reforested lignite-rich mine soils. Geoderma 86, 123-142.
790
791 Rumpel, C., Kogel-Knabner, I., Knicker, H., Huttl, R.F., 2000a. Composition and distribution of
792 organic matter in physical fractions of a rehabilitated mine soil rich in lignite-derived carbon.
793 Geoderma 98, 177-192.
794
795 Rumpel, C., Kogel-Knabner, I., Bruhn, F., 2002. Vertical distribution, age, and chemical composition
796 of organic carbon in two forest soils of different pedogenesis. Org. Geochem. 33, 1131-1142.
797
798 Rumpel, C., Kogel-Knabner, I., 2004. Microbial use of lignite compared to recent plant litter as
799 substrates in reclaimed coal mine soils. Soil Biol. Biochem. 36, 67-75.
800

Rumpel, C., Skjemstad, J.O., Knicker, H., Kögel-Knabner, I., Hüttl, R.F., 2000b. Techniques for the differentiation of carbon types present in lignite-rich mine soils. Org. Geochem. 31, 543-551.

Schmidt, M.W.I., Knicker, H., Hatcher, P.G., Kogel-Knabner, I., 1997. Improvement of ^{13}C and ^{15}N CPMAS NMR spectra of bulk soils, particle size fractions and organic material by treatment with 10% hydrofluoric acid. Eur. J. Soil Sci. 48, 319-328.

Shrestha, R.K., Lal, R., 2011. Changes in physical and chemical properties of soil after surface mining and reclamation. Geoderma 161, 168-176.

Stuiver, M., Polach, H.A., 1977. Reporting of ^{14}C data - Discussion. Radiocarbon 19, 355-363. DOI 10.1017/S0033822200003672

Tabatabai, M.A., Bremmer, J.M., 1969. Use of p-nitrophenyl phosphate for assay of soil phosphatase activity. Soil Biol. Biochem. 1, 301-307.

Tabatabai, M.A., Bremmer, J.M., 1970. Arylsulfatase activity of soils. Soil Sci. Soc. Am. J. 34, 225-229.

ter Braak, C.J.F., Smilauer, P., 2002. CANOCO Reference manual and CanoDraw for Windows User's guide: Software for Canonical Community Ordination (version 4.5). Ithaca, NY, USA, 500 p.

Thielemann, T., Schmidt, S., Peter Gerling, J., 2007. Lignite and hard coal: Energy suppliers for world needs until the year 2100 — An outlook. Int. J. Coal Geol. 72, 1-14.

Thiery, V., Sokol, E.V., Masalehdani, N-N., Guy, B., 2013. La combustion des terrils. Géochronique, Bureau de recherches géologiques et minières, 2013, 127, pp.23-25. hal-00880725.

Tran, C.K.T., Rose, M.T., Cavagnaro, T.R., Patti, A.F., 2015. Lignite amendment has limited impacts on soil microbial communities and mineral nitrogen availability. Appl. Soil Ecol. 95, 140-150.

Wang, K., Fu, X., Qin, Y., Sesay, S., 2011. Adsorption characteristics of lignite in China. J. Earth Sci. 22, 371-376.

WRB, 2015. World reference base for soil resources 2014, update 2015. International soil classification system for naming soils and creating legends for soil map. World Soil Resources Reports No. 106. FAO, Rome.

Figure captions

Fig. 1. PCA of physico-chemical characteristics of control and spoil heap soils (squares are control soils (C) from natural site included in the analysis as additional and passive observations). Legend of soil samples: 1st number refers to spoil heap level/belt (1 to 4); 2nd number refers to the composite soil replicate; example: 2.3. refers to the third composite sample of the level 2 of the spoil heap.

Fig. 2. PCA of ^{13}C CPMAS NMR signals of control and spoil heap soils (squares are control soils (C) from natural site included in the analysis as additional and passive observations). Legend of soil samples: 1st number refers to spoil heap level/belt (1 to 4); 2nd number refers to the composite soil replicate; example: 2.3. refers to the third composite sample of the level 2 of the spoil heap.

Fig. 3. PCA of biological activities of control and spoil heap soils (squares are control soils (C) from natural site included in the analysis as additional and passive observations). Legend of soil samples: 1st number refers to spoil heap level/belt (1 to 4); 2nd number refers to the composite soil replicate. example: 2.3. refers to the third composite sample of the level 2 of the spoil heap.

Fig. 4. Partitioning of the net variance in the response data (microbiological) into the contribution of the two subsets of environmental variables (i.e. physico-chemical and 13C NMR quality) on the whole (heap and controls from natural site) and the reduced datasets (heap only) and on each individual microbial variable (heap only).

Supplementary files

File “Supplementary figures” includes :

- **Supplementary Figure S1.** Aerial view of the Armand spoil heap (Peypin, France) and location of the collected soil samples. The sampling strategy on the heap and the making of the composite samples are also detailed. Satellite image from Google Earth.

- **Supplementary Figure S2.** Typical a) control (natural site) and b) spoil heap profiles at the Armand site. Names are given after WRB (2015).
- **Supplementary Figure S3.** Coefficients of variation of the different variables of the Armand spoil heap.
- **Supplementary Figure S4.** USDA Diagram of textural classification of surface (A) horizons of the Armand spoil heap and control (natural site) soils and comparison with Kirbon lignite outcrop soils (Kirbon hamlet, Trets, Bouches du Rhône, France) with and without lignite A and A/C horizons*; * data from Clouard et al. (2014); Textural diagram from www.nrcs.usda.gov/wps/portal/nrcs/detail/soils.

File "Supplementary tables" includes :

- **Supplementary Table S1.** XRD analysis of minerals in soil samples.1/0 means presence / absence.
- **Supplementary Table S2.** Selected variables in physico-chemical and ^{13}C NMR subsets of data. X1 and X2 refer to the variables used respectively for the physico-chemical and ^{13}C NMR fractions of variance partitioning.

884

885 **Tables**

886

887

888 **Table 1. Physico-chemical characteristics of spoil heap and control (natural site) soils. Means (± SE, n=3 for level 1 and n=4 for level 2, 3, 4 and**
889 **control) with different letters within a column are significantly different based on Kruskal-Wallis *post hoc* test ($P < 0.05$)**

Level	pH	Carbonates ($g\ kg^{-1}$)	Corg (%)	Ntot (%)	C/N ratio	Clay ($g\ kg^{-1}$)	Silt ($g\ kg^{-1}$)	Sand ($g\ kg^{-1}$)	CEC ($cmol^{+}\ kg^{-1}$)
Level 1	8.53 ± 0.1 a	656 ± 120 a	5.1 ± 2.2 a	0.5 ± 0.2 a	10.1 ± 1.6 a	135 ± 15 c	346 ± 55 b	520 ± 66 a	25.0 ± 6 b
Level 2	8.47 ± 0.08 a	524 ± 95 abc	8.0 ± 2.7 a	0.6 ± 0.2 a	14 ± 2.2 ab	169 ± 7 b	389 ± 102 ab	442 ± 108 a	34.2 ± 8.4 ab
Level 3	8.46 ± 0.15 a	562 ± 106 abc	9.7 ± 3.1 a	0.7 ± 0.1 a	14.1 ± 3 b	166 ± 18 bc	395 ± 19 ab	439 ± 31 ab	37.1 ± 2.8 a
Level 4	8.50 ± 0.05 a	461 ± 16 b	11.3 ± 3.3 a	0.6 ± 0.2 a	19.7 ± 2.1 b	175 ± 21 b	439 ± 24 a	387 ± 33 b	40.4 ± 3 a
Controls	8.40 ± 0.11 a	400 ± 56 c	10.4 ± 2.4 a	0.7 ± 0.3 a	15.2 ± 3.6 ab	342 ± 60 a	436 ± 85 ab	222 ± 32 c	39.1 ± 6.7 a

890

891

892

893 **Table 2. Absolute intensities (mg g^{-1}) derived from the ^{13}C CPMAS NMR spectra of spoil heap and control (natural site) soils. Means (± SE, n=3 for**
894 **level 1 and n=4 for levels 2, 3, 4 and controls) with different letters within a column are significantly different based on Kruskal-Wallis *post hoc* test**
895 **($P < 0.05$)**

Level	Alkyl C	Methoxyl C	*O*-alkyl C	Aromatic C	Phenolic C	Carboxyl C	Ratio A	Aromatic Index
Level 1	9.4 ± 2.65 b	2.6 ± 1.08 a	13.1 ± 4.65 b	8.6 ± 4.52 b	2.5 ± 1.3 a	3.2 ± 0.99 a	1.1 ± 0.23 b	0.2 ± 0.07 a
Level 2	20.2 ± 2.95 a	4.8 ± 2.06 a	19.5 ± 2.71 b	23.7 ± 9.67 a	3.5 ± 0.64 a	5.4 ± 0.67 ab	1.8 ± 0.42 a	0.3 ± 0.1 a
Level 3	21.6 ± 5.61 a	3.7 ± 0.78 a	23.3 ± 9.41 b	23.6 ± 4.81 a	3.1 ± 1.35 a	5.4 ± 1.58 b	1.6 ± 0.37 ab	0.3 ± 0.02 a
Level 4	24.9 ± 7.79 a	4.3 ± 0.97 a	20.9 ± 5.04 b	32.2 ± 10.99 a	3.3 ± 1.55 a	6.1 ± 1.15 ab	2.2 ± 0.86 a	0.3 ± 0.08 a
Controls	18.9 ± 5.15 a	6.1 ± 2.4 a	32.9 ± 7.69 a	9.9 ± 2.46 b	3.3 ± 0.65 a	6.7 ± 1.31 a	0.7 ± 0.17 b	0.1 ± 0.01 b

896
897
898
899
900
901
902
903
904
905
906
907
908
909
910
911
912
913
914
915
916

Table 3. Enzymatic activities (basic phosphatase, acid phosphatase, β-glucosidase, arylsulfatase, arylamidase, lipase and FDA hydrolase), basal respiration measured by Oxitop® system and functional diversity measured by Biolog® system in the different levels (1, 2, 3 and 4) on the spoil heap and in the control (natural site) soils. Means (± SE, n=3 for level 1 and n=4 for levels 2, 3, 4 and controls) with different letters within a column are significantly different based on Kruskal-Wallis *post hoc* test ($P < 0.05$).

Level	BPH (mU g^{-1}MS)	APH (mU g^{-1}MS)	β-glu (mU g^{-1}MS)	ArylS (mU g^{-1}MS)	ArylN (mU g^{-1}MS)	FDL (mU g^{-1}MS)	FDA (mU g^{-1}MS)	Oxitop BR (mg O_2 g^{-1} d^{-1})	Biolog (AWCD)
Level 1	81.26 ± 29.37 a	64.76 ± 19.68 b	5.71 ± 1.59 ab	74.30 ± 61.01 b	10.72 ± 5.51 a	0.34 ± 0.18 a	38.36 ± 8.07 a	1.79 ± 0.73 b	0.34 ± 0.14 a
Level 2	66.72 ± 25.5 a	61.18 ± 5.32 b	5.00 ± 0.96 b	75.65 ± 11.32 b	11.99 ± 2.93 a	0.41 ± 0.16 a	35.66 ± 7.85 a	1.75 ± 0.45 b	0.51 ± 0.18 a
Level 3	86.90 ± 4.15 a	67.40 ± 9.61 b	5.25 ± 0.43 b	87.98 ± 12.15 b	13.42 ± 3.98 a	0.84 ± 0.43 a	41.11 ± 7.76 a	2.24 ± 0.73 ab	0.47 ± 0.21 a
Level 4	92.65 ± 15.25 a	62.20 ± 7.23 b	4.70 ± 1.1 b	77.82 ± 17.8 b	12.66 ± 2.64 a	0.72 ± 0.57 a	30.21 ± 10.27 a	3.00 ± 1.69 a	0.42 ± 0.20 a
Controls	101.78 ± 36.29 a	170.70 ± 34.46 a	6.95 ± 0.45 a	368.70 ± 58.03 a	8.66 ± 2.72 a	0.80 ± 0.46 a	46.81 ± 9.55 a	2.93 ± 0.21 ab	0.48 ± 0.19 a

Table 4. Pearson correlation values obtained between microbial activities and environmental variables in soil samples of the Armand spoil heap. Values in bold are significant at $P < 0.05$.

	Microbial activity								
Environmental variables	BPH	APH	β-glu	ArylS	ArylN	FDL (lipase)	FDA	Oxitop	AWCD
Carbonates	-0,27	0.25	0.34	0.36	0.02	0.03	0.17	-0.25	-0.10
Corg	0.12	0.14	0.08	0.15	0.23	0.16	0.13	0.15	0.23
N	0.08	0.48	0.47	0.43	0.07	0.28	0.42	0.04	0.35
C/N	0.09	-0.24	-0.33	-0.14	0.32	-0.05	-0.27	0.32	0.02
Clay	-0.02	-0.02	-0.16	0.09	0.15	0.12	-0.47	**0.53**	0.29
Silt	-0.14	0.05	-0.18	0.01	-0.24	0.29	-0.25	0.29	0.11
Sand	0.12	-0.04	0.19	-0.04	0.16	-0.28	0.33	-0.39	-0.17
CEC	0.07	0.20	-0.07	0.15	0.10	0.34	0.03	0.27	0.28
Alkyl-C	0.09	0.09	-0.14	0.11	-0.02	0.36	-0.35	0.68	0.28
Methoxyl-C	-0.23	-0.11	0.43	-0.04	0.22	-0.30	-0.11	0.18	0.03
O-alkyl-C	0.28	0.38	0.17	0.27	0.37	0.19	0.31	0.22	0.17
Aromatic-C	-0.02	-0.14	-0.45	-0.18	-0.07	0.15	-0.42	0.50	-0.16
Phenolic-C	-0.12	0.06	-0.05	-0.21	**-0.54**	0.41	-0.23	0.23	0.27
Carboxyl-C	0.24	0.21	-0.04	0.09	0.17	0.25	-0.02	0.28	0.17
Ratio A	-0.16	-0.33	**-0.53**	-0.27	-0.28	0.15	**-0.71**	0.62	-0.14
AI	-0.14	-0.33	**-0.58**	-0.36	-0.18	0.13	-0.46	0.22	-0.24

Table 5. Multiple linear regressions between microbial responses and environmental variables (^{13}C NMR OM quality and physico-chemical variables).

	β-coefficient						
Model	Alkyl C	Methoxyl C	*O*-Alkyl C	Phenolic C	Carboxyl C	Aromatic index	Adj. R^2
BPH	0.41ns	-0.58ns	0.54ns	-0.56ns			0.15ns
APH		-0.29ns	0.51ns			-0.33ns	0.15ns
Glu		-0.54*			0.52*	-0.81**	0.59**
ArylS				-0.51ns	0.69.	-0.57.	0.20ns
Aryln				-1.14***	1.12**	-0.44**	0.86***
FDL	0.70*	-0.66*					0.35*
FDA	-0.66*		0.69*			-0.25ns	0.44*
BR	1.07**	-0.26ns			-0.37ns		0.47*
AWCD	0.41ns					-0.38ns	0.08ns

	β-coefficient						
Model	Carbonates	N	C/N	Clay	Sand	CEC	Adj. R^2
BPH	1.31**	-0.28ns	0.57ns		0.91.	1.60*	0.40.
APH	0.63ns	0.36ns	-0.13ns			0.56ns	0.26ns
Glu	0.45.	0.56*					0.32*
ArylS	1.10*	0.31ns	0.29ns			0.64.	0.41*
Aryln	0.59ns		0.76.				0.13ns
FDL	0.59ns					0.77.	0.16ns
FDA		0.46.		0.50*			0.34*
BR				0.03*			0.23*
AWCD		0.35ns					0.05ns

*** P < 0.001; ** P < 0.01; * P < 0.05; · P < 0.1; ns: not significant.

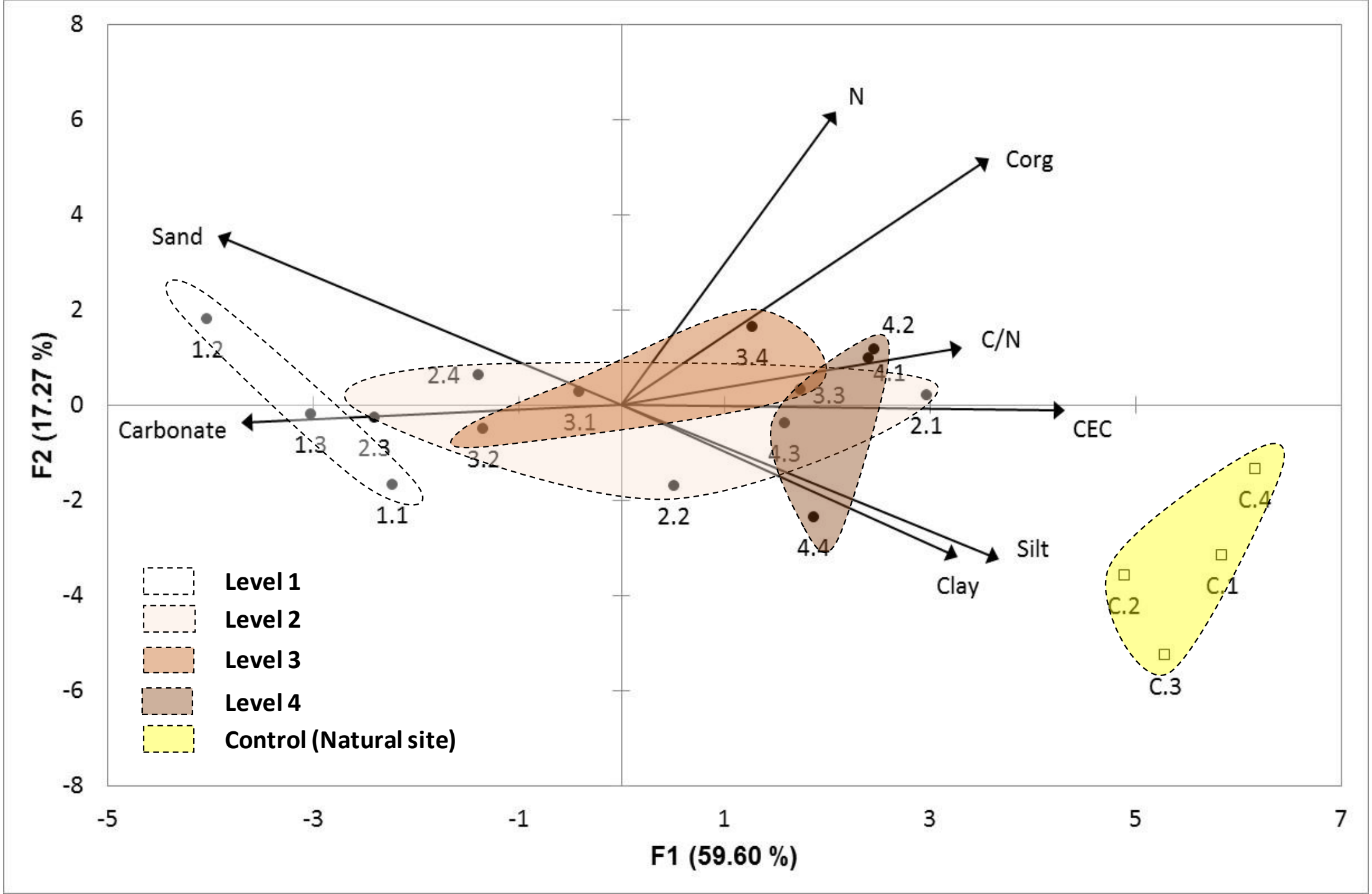
N
Corg
Sand
C/N
Carbonate
CEC
Silt
Clay
1.2
2.4
3.4
4.2
4.1
3.3
3.1
2.1
1.3
2.3
3.2
4.3
1.1
2.2
4.4
C.4
C.1
C.2
C.3
Level 1
Level 2
Level 3
Level 4
Control (Natural site)
F2 (17.27 %)
F1 (59.60 %)
8
6
4
2
0
-2
-4
-6
-8
-5
-3
-1
1
3
5
7

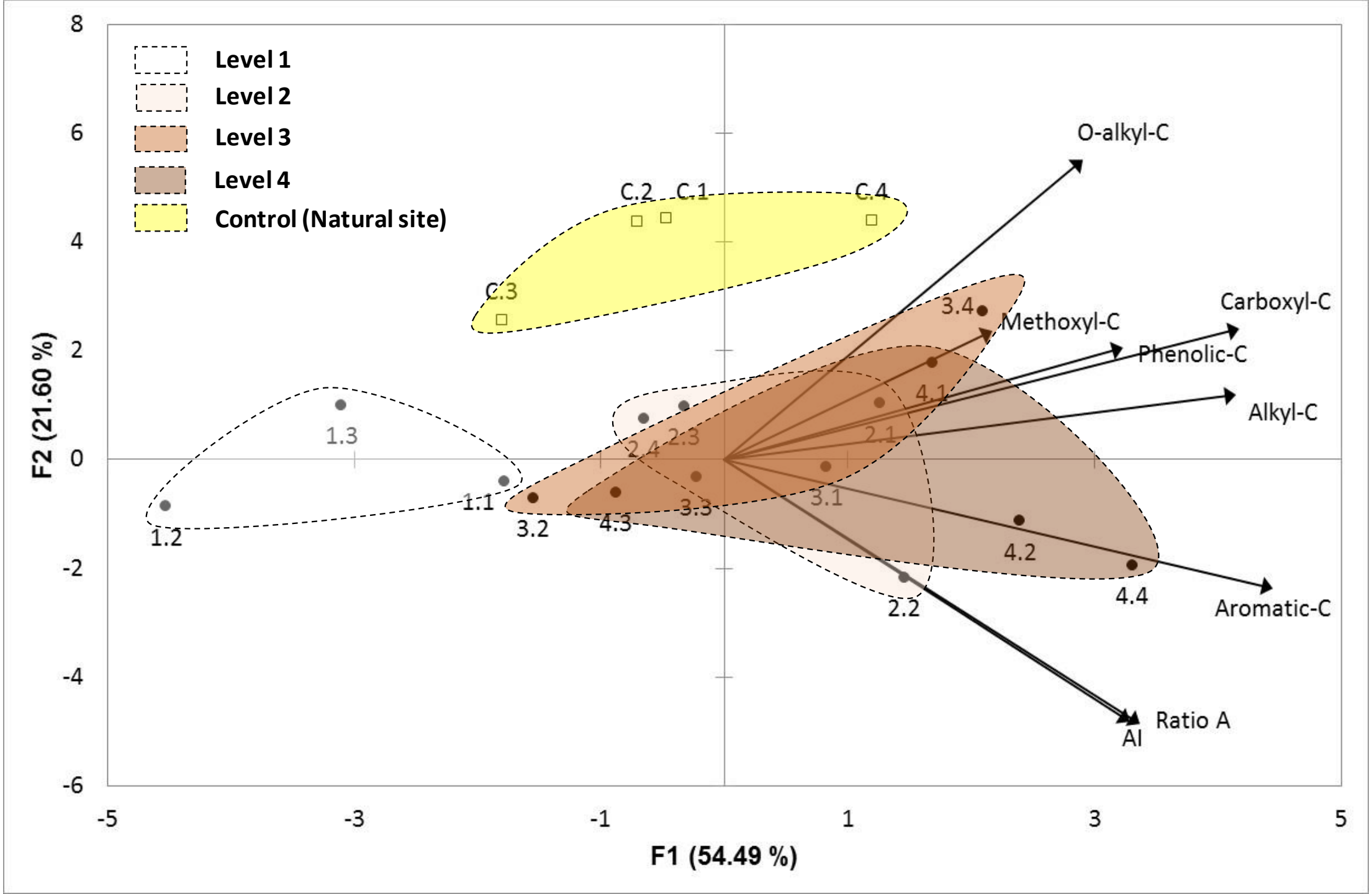
Level 1
Level 2
Level 3
Level 4
Control (Natural site)
C.2
C.1
C.4
C.3
O-alkyl-C
Carboxyl-C
Methoxyl-C
Phenolic-C
Alkyl-C
Aromatic-C
Ratio A
AI
3.4
4.1
2.3
2.4
2.1
1.3
1.1
1.2
3.2
4.3
3.3
3.1
4.2
4.4
2.2
F2 (21.60 %)
F1 (54.49 %)
8
6
4
2
0
-2
-4
-6
-5
-3
-1
1
3
5

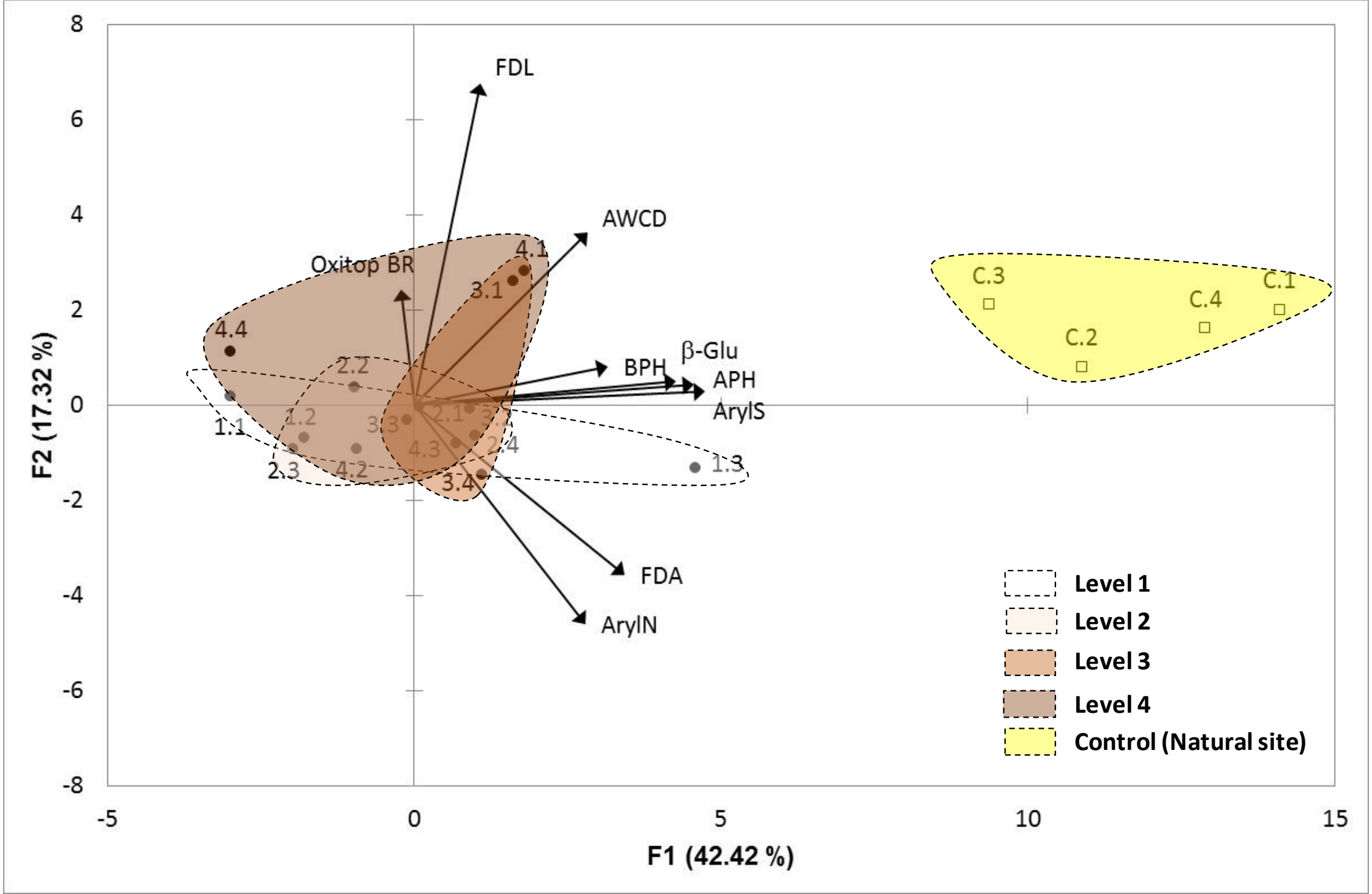
FDL
AWCD
Oxitop BR
β-Glu
BPH
APH
ArylS
ArylN
FDA
4.1
3.1
4.4
2.2
1.1
1.2
3.3
2.1
3.2
2.4
4.3
2.3
4.2
3.4
1.3
C.3
C.1
C.4
C.2
Level 1
Level 2
Level 3
Level 4
Control (Natural site)
F2 (17.32 %)
F1 (42.42 %)
8
6
4
2
0
-2
-4
-6
-8
-5
0
5
10
15

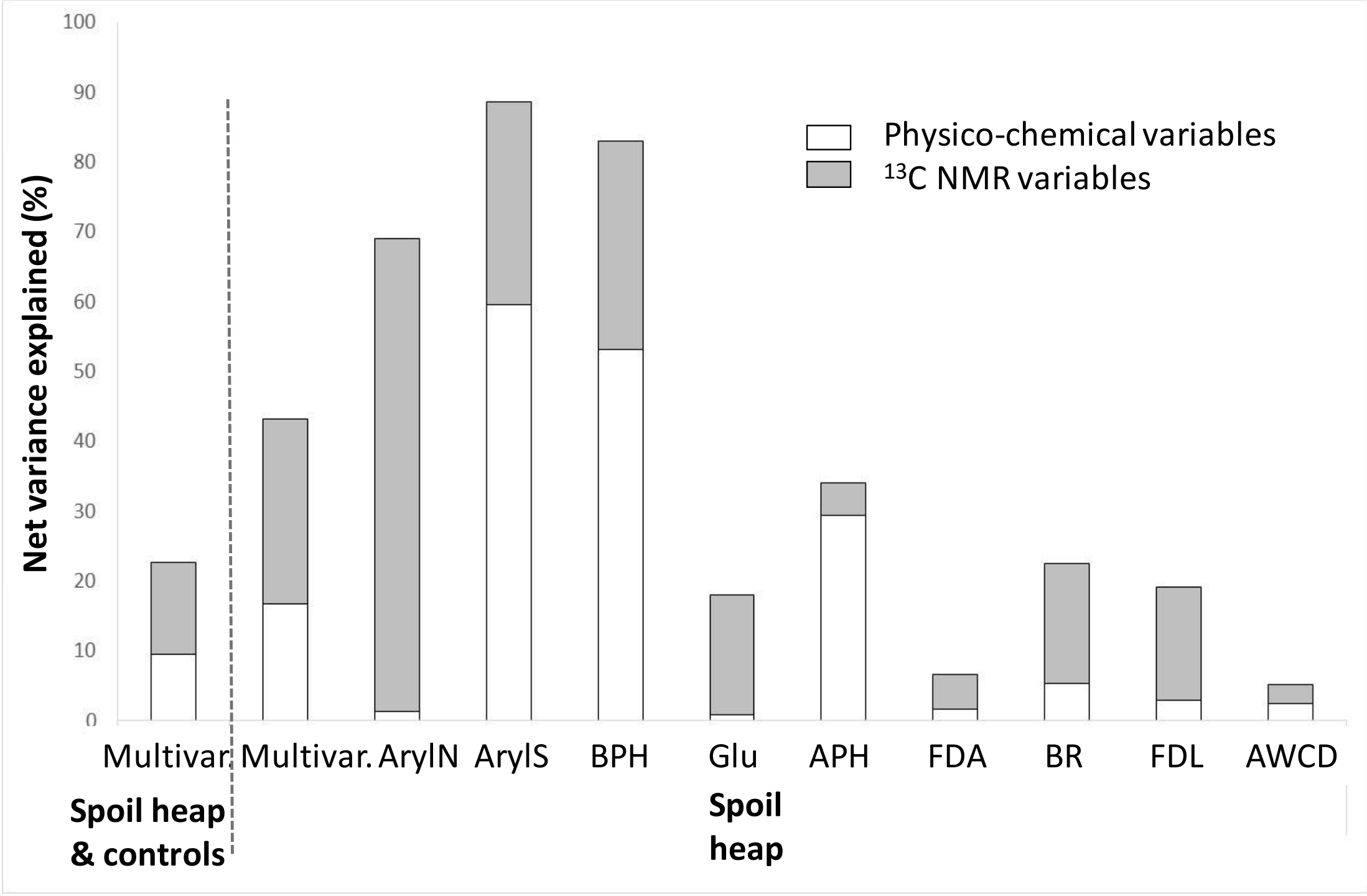
Net variance explained (%)
100
90
80
70
60
50
40
30
20
10
0
Physico-chemical variables
13C NMR variables
Multivar.
Multivar.
ArylN
ArylS
BPH
Glu
APH
FDA
BR
FDL
AWCD
Spoil heap & controls
Spoil heap

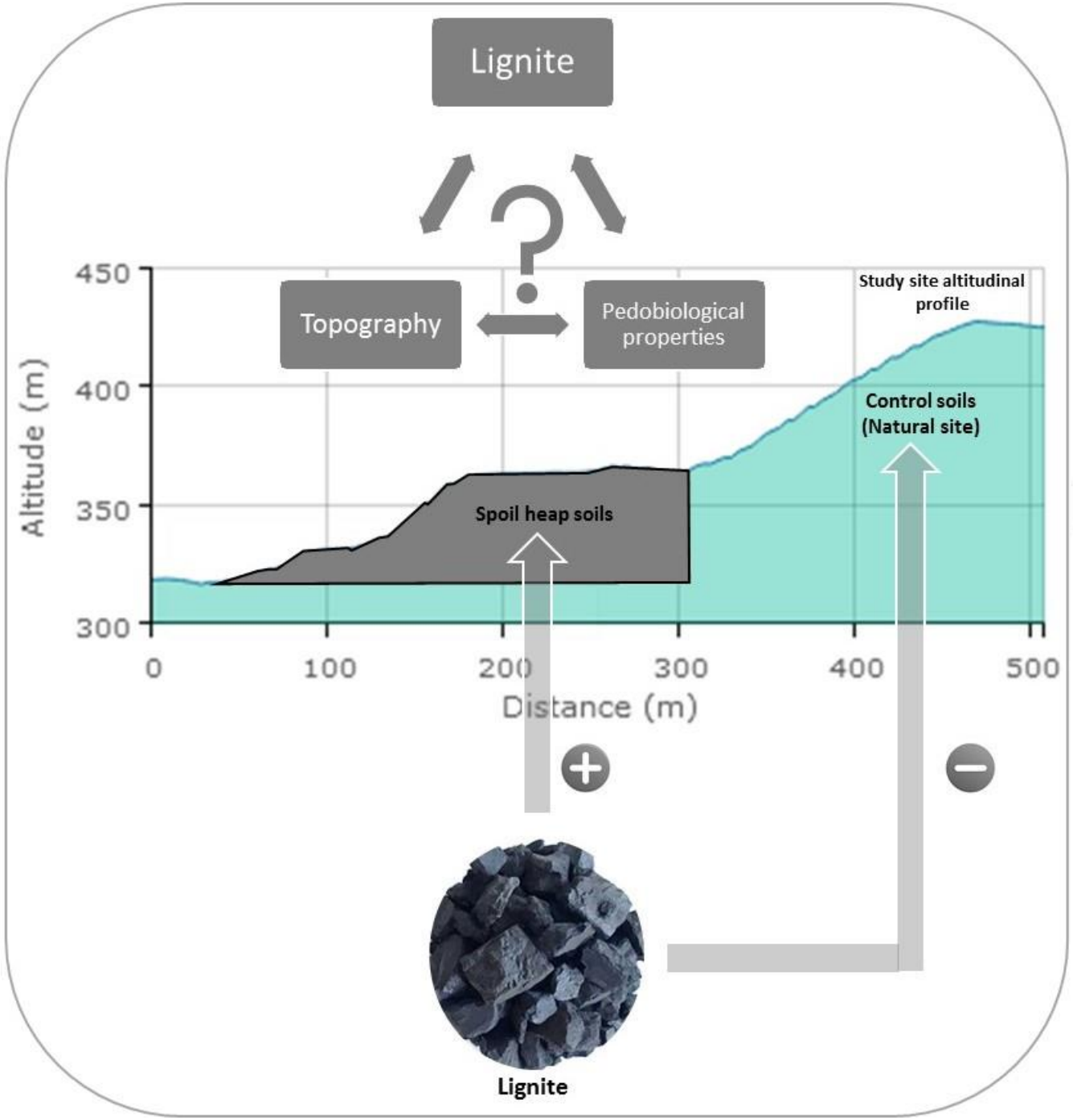

Main results

Slope discriminate :
particle size, CEC, carbonate

Patchy distribution of :
Lignite, microbial activities

Negative effects of lignite on microbial parameters